SOVIET PHYSICS

USPEKHI

A Translation of Uspekhi Fizicheskikh Nauk

SOVIET PHYSICS USPEKHI (Russian Vol. 90, Nos. 3 and 4) MAY-JUNE 1967

551.510.535

THE OUTER IONOSPHERE AND ITS TRANSITION TO THE INTERPLANETARY MEDIUM

Ya. L. AL'PERT

Institute of Terrestrial Magnetism, Ionosphere, and Radio Wave Propagation,
Academy of Sciences, U.S.S.R.

Usp. Fiz. Nauk 90, 405–433 (November, 1966)

INTRODUCTION

MANY experimental results obtained in recent years allow us to attempt to examine the general picture of the construction of the outer ionosphere up to the uppermost limit as depicted by these data.

This is the region of the near-earth plasma, the existence of which has been known for many years. It was deduced a priori long ago from general considerations concerning the structure of the earth's atmosphere and its interaction with the solar radiation, and its investigations began with studies of whistlers in 1953, when it was shown [1] that at distances 18—19 thousand kilometers from the earth the electron concentration is of the order of 400—600 el/cm^3. In 1957 and 1958, the first curves showing the distribution of the electron concentration up to an altitude of the order of 13,000 km [2] and 25,000 km [3] were obtained with the aid of whistlers. At the same time, it was stated in the literature that the earth has a thick outer ionosphere consisting of ionized hydrogen and extending to altitudes of the order of eight earth's radii (R_0), where it has a sharp boundary, beyond which interplanetary winds blow [4]. This notion is in fairly good agreement with modern concepts. It has turned out, however, that at distances 15—25 thousand km from the earth the processes occurring in the near-earth plasma are more complicated. Apparently the so-called "knee" is formed here from time to time [5,6].

It is curious to note in this connection that relatively recently it was still stated that a previously unknown plasma sheath exists around the earth in the altitude region 2—20 thousand km, and its existence was deduced on the basis of an investigation which, as will be shown below, generally contradicts the published data [10].

As a result of an analysis of the state of the near-earth plasma it becomes advantageous, for a number of reasons given below, to regard the region of the knee, i.e., the region of altitudes (3—4.5) R_0, as the boundary of the outer ionosphere. On the other hand, the region from (3—4.5) to (8—10) R_0—the magnetosphere—is the region of transition to the interplanetary medium.

We point out also the great variety of designations of the outer ionosphere, which cause a certain degree of confusion and which lack sufficient physical foundation. Thus, for example, it is called by different authors "protosphere," "protonosphere," "exosphere," "magnetosphere," "plasmasphere," and "geocorona." The last term is particularly inappropriate, since the physical conditions in the outer ionosphere differ greatly from the physical conditions existing even at the boundary of the solar corona. Apparently, in view of the ever growing research on the near-earth plasma, it would be advisable to establish a single term for it—the outer ionosphere.

Research with the aid of whistlers and low frequency waves of other types has by now become a very important source of information on the near-earth plasma. The results obtained with it permit a deep insight into its main properties—the effective temperature of the medium, the particle velocity distribution, the concentration of the electrons and ions of different sorts, etc. [7,8,9]. The corresponding published experimental data will be used below. However, we present only a brief analysis of the theory

of these methods. Theoretical questions will be separately treated in a special article.*

An important role in the study of the outer ionosphere (its lower part) is also played by results of an investigation of the energy spectra of "incoherent" scattering of radio waves by electron fluctuations. Experimental data on incoherent scattering of radio waves have disclosed important properties of the outer ionosphere [11,12,13]. These experiments have revealed the fundamental fact that in the region of altitudes 300—700 km the electron temperature differs from the ion temperature by 3—4 times in some cases, and have yielded data on the composition of the ionosphere, its concentration, etc. Naturally, an appreciable contribution was made by various measurements with satellites and rockets. We shall use below charged-particle altitude distributions obtained by different methods [14-19]. An important result of these experiments is the measurement of the hydrogen and helium contents in the outer ionosphere [20,21]. Of great interest are also the measured concentrations of the neutral particles above 5—6 thousand km [22], which have in part led the author to the conclusions presented below concerning the boundary of the ionosphere, and concerning the "sweeping out" of particles from the higher-lying regions of the magnetosphere.

However, some measurements with rockets and satellites, using so-called ion traps, have led to incorrect conclusions [10,21]. This is due is in particular to the fact that the conversion of the measured fluxes of particles captured in probes into the correct values of the density of the surrounding medium calls for great caution and is frequently unambiguous. The question of the status of the theory of the corresponding measurements will be discussed briefly below.

1. ALTITUDE VARIATION OF THE CHARGED-PARTICLE CONCENTRATION UP TO 50—100 THOUSAND KILOMETERS ABOVE THE EARTH

The aggregate of the experimental data that give a general idea of the altitude distribution of the charged-particle concentration in the outer ionosphere is shown in Figs. 1 and 2. The curves in these figures were obtained from different experiments. In order to reveal certain singularities of the altitude distribution, the results of individual investigations are given in Figs. 3—6. The generalized curves of Figs. 1 and 2 contain a large amount of information: they include the results of numerous experiments carried out in different periods of time by various methods. A careful examination of these figures leads directly to a number of general conclusions concerning the

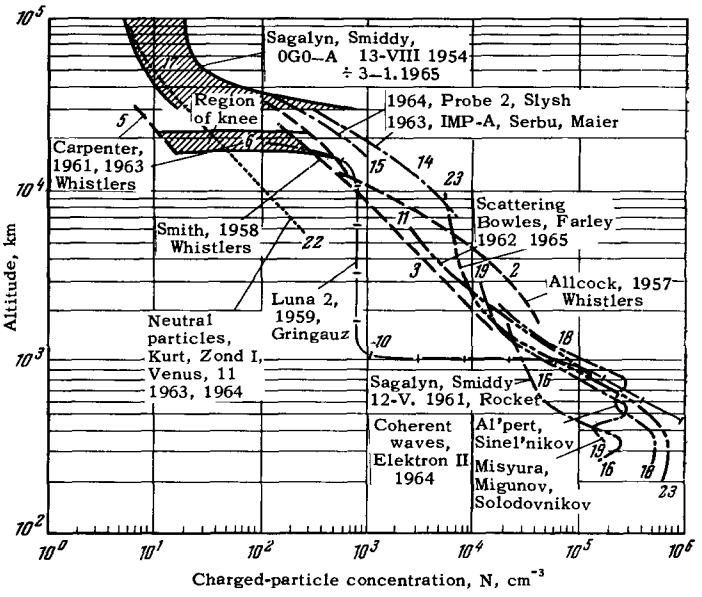

FIG. 1

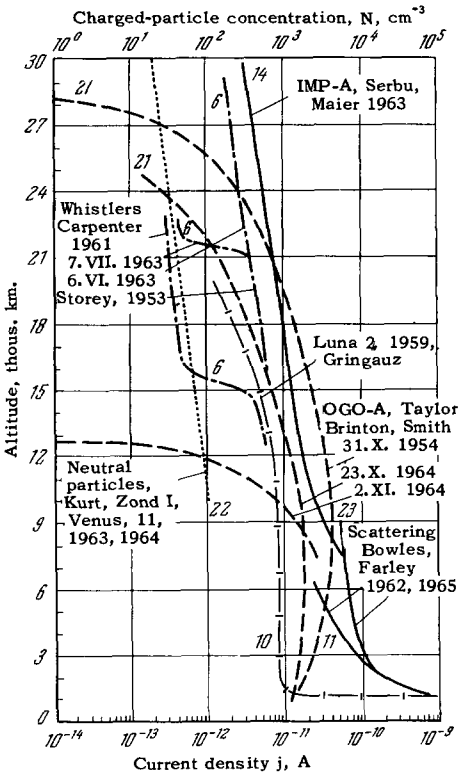

FIG. 2

structure of the outer ionosphere. The curves on Figs. 1 and 2 characterize the results of measurements during different parts of the day, in different years, and in regions with different geographic and and magnetic coordinates. Each curve is tagged with the authors of the corresponding results, the type of satellite or rocket, the year of the measurement, and the number of the literature reference.

*This paper is now in press.

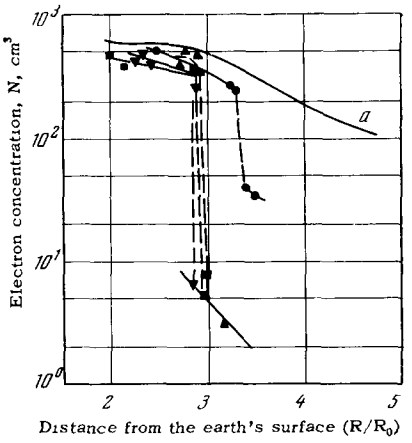

FIG. 3

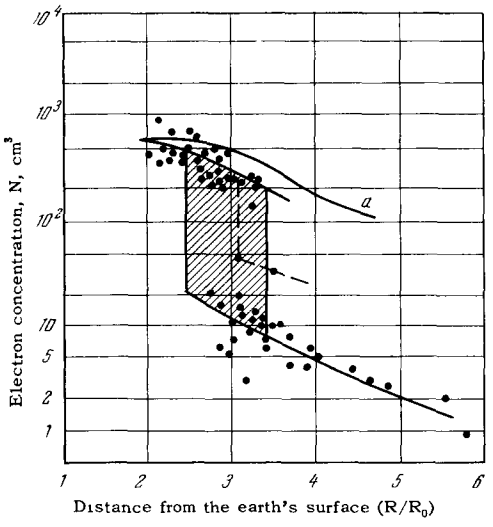

FIG. 4

Let us examine Fig. 1 first. The general property of all the data, with the exception of curve 10, which will be discussed separately below, is that the curves form a single channel: the concentration of the charged particles in general decreases smoothly and slowly with altitude, starting with Z ~ 800—1000 km to Z ~ 30—40 thousand km from the surface of the earth. Singularities appear in the N(Z) dependence at altitudes of 15—25 thousand km, above 30—40 thousand km, and also below 700—800 km.

It was observed with the aid of whistlers that at altitudes Z ~ 15—25 thousand km, during the periods of even relatively weak magnetic disturbances (index $k \gtrsim 2$), the electron concentration decreases very rapidly, almost "jumplike," by a factor of several thousand times, while the altitude decreases in some cases only by 600—700 km. This phenomenon was called the "knee" [5]. The region of the knee, according to the latest data [6], is outlined in Figs. 1 and 4. In Fig. 2, the altitude dependence of the charged particles is plotted in a linear altitude scale, showing how the individual N(Z) curves vary in the region of the knee. Figures 3 and 4 show primary research data on the knee, taken from [6]. For comparison, Figs. 3 and 4 show also an electron-concentration plot obtained in these experiments during the periods when the knee was not observed (curve a).

Above 30 thousand km, we used in Fig. 1 the results of measurements of the concentration of low-energy ("thermal") positive ions with the aid of a spherical electrostatic analyzer on the orbital geophysical laboratory OGO-A [17]. Notice should be taken here of two important properties of the results of these experiments. In the next section we shall consider one more of their singularities. The values of the concentration change strongly from measurement to measurement and lie within the limits of the band shown in Fig. 1. From 40—50 thousand km up to 160 thousand km, at which the measurements were made, the concentration is almost constant and fluctuates approximately in the range 5—10 particles/cm^3. We note that the concentration of the particles with higher energies (~ 400—1300 eV) is of the order of one per cm^3.

It is easy to note now that the upper limit of the concentrations measured in these experiments is quite close to the upper limit of the electron concentrations obtained with the aid of whistlers, and is also in good agreement with the data of other measurements [14,15]. On the other hand, the lower limit falls in the region of minimal values of the region of the knee. Thus, it appears likely that the spread in the values of the concentration obtained on the OGO-A [17] is due to the same cause as the phenomenon of the knee, and is connected with the fact that above 15—20 thousand km, during the "disturbed" periods, the concentration of the charged particles decreases. Attention is called here to line 22 shown of Figs. 1 and 2, i.e., to the variation of the concentration of neutral particles, obtained with the rockets "Zond I" and "Venus II" by measuring the intensity of scattering by hydrogen—the L_α line (1216 Å) of solar emission [22]. Above 15—20 thousand km, the concentration of the neutral particles agrees closely with the minimum values of the concentration of the charged particles.* (In Sec. 3, where certain measurement methods are briefly reviewed, we discuss the need for correcting somewhat the results of the measurements obtained with the aid of whistlers.)

The foregoing circumstances allow us to assume that during the periods of "disturbances" the particles, as it were, are "swept" into the lower regions of the ionosphere. The particles "fall out" and as a result additional belts, electric fields, vibrational

*In [62], using coherent frequencies, it was also found that on the average N ~ (1–2) × 10^3 el/cm^3 at an altitude Z ~ 13 thousand km.

plasma structure, and other complicated plasma phenomena can occur. It is not excluded that the "breakup" of the regular structure of the lower regions of the ionosphere, observed during the period of the so-called strong "ionospheric storms," is the clearest manifestation of these phenomena.

It will be shown in the next section that in the region of the near-earth plasma referred to above, i.e., at altitudes (3—3.5) R_0 and higher over the earth's surface, the Maxwellian distribution is also strongly violated, there is apparently no quasi-neutrality, and large electric fields are produced. All this indicates that the plasma here is in a nonstationary state and is governed essentially by the particle streams that fall on the earth from the outside. For these reasons, we believe a correct definition of the boundary of the ionosphere to be the region of formation of the knee, where the concentration N(Z) has two branches, one of them corresponding to the minimum values of N, agrees closely with the concentration of the neutral particles, as is perfectly natural.

With such a definition of the boundary of the ionosphere, it becomes apparently possible to describe the ionization balance by means of a single equation for the formation of the ionosphere, which will be considered in Sec. 5.

The region of the nonstationary state of the near-earth plasma (above (3—3.5) R_0) is the upper part of the magnetosphere. It is here that the magnetic field of the earth begins to break up even under undisturbed conditions, inasmuch as frequently $H_0^2/8 \sim (N_0 M v_0^2/3)$. At distances (8—10) R_0 from the earth, as is well known, the regular magnetic field of the earth plays already a minor role, with fields of the fluctuation type prevailing, such as "frozen in" field of plasma bunches. It is here where the interplanetary plasma proper begins.

In the region of altitudes from 700—800 km to 10—15 thousand km, the differences in the variation of the concentration N(Z) in different experiments is due to a number of causes: principal among these is apparently the change in the external conditions of the experiments (time, coordinates, magnetic field). Individual experiments or series of experiments frequently have different singularities, evidencing the complicated dynamics of the particles in the ionosphere, the frequent absence of a smooth variation of N(Z), and in general the great variety of states of the near-earth plasma. For example, Fig. 5, which shows individual curves of the altitude variation of the electron concentration, obtained in Peru by incoherent scattering of radio waves during approximately the same interval of time (15:24—15:36) on 1, 2, and 3 February 1965 [23], and at altitudes 4—8 thousand km, the variation of N(Z) is patently quasi-periodic. On the other hand, in the same experiments at lower altitudes, the N(Z) plotted during a 24-hour period

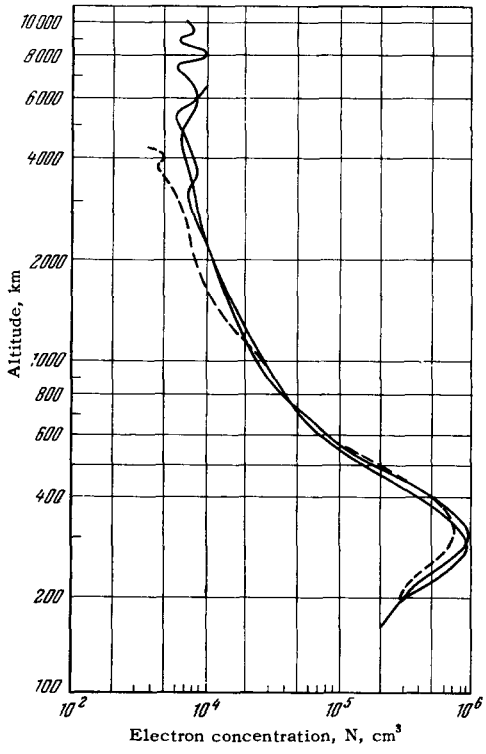

FIG. 5

(from the 2 to 3 February, 1965) above 800 km, converge to a single node (Fig. 6), indicating that the electron concentration had an almost irregular value during the day. Below 700—800 km, in the region of the principal maximum of the ionosphere, the N(Z)

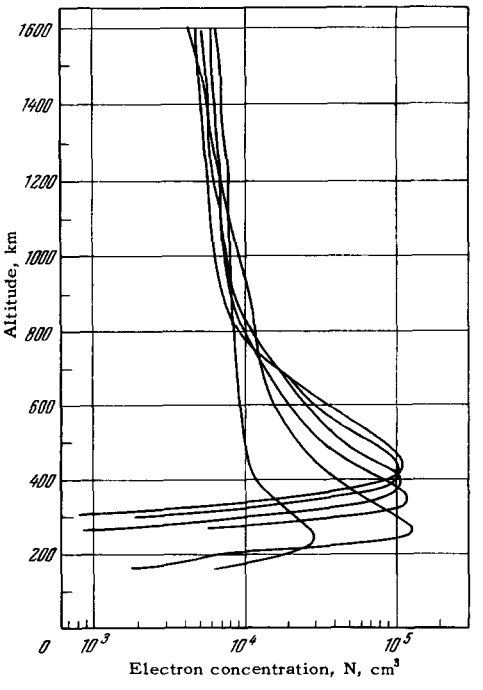

FIG. 6

curves can, naturally, differ greatly because of the influence of the diurnal variation. (see Figs. 1 and 6). However, even in this region of altitudes one observes in different experiments certain distinguishing features. For example, in investigations using coherent waves with the aid of the satellite "Elektron" in Moscow [18,19] and in Kharkov [19], the average altitude variation of N(Z) has additional maxima (see Fig. 1, curves 18 and 19). The nature of these maxima is not clear. They must, naturally, not be regarded as the result of a regular formation of additional layers above the principal maximum of the ionosphere N(Z). They are apparently due to the complicated dynamics of the upper ionosphere and point to the presence at different points of a preferred direction (sign) of the horizontal gradient of the electron concentration and to a predominant direction of the wind. Above the principal maximum $N_{MAF}F^2$, and in other experiments, additional maxima are also observed [24,25], the origin of which can, however, be connected with other factors (see, for example, [26]). In the next section we shall present data indicating that the lower part of the outer ionosphere—approximately 400—800 km—has also other peculiarities, which offer evidence of the variety of the processes occurring in it and in general of the "activity" of this region of the near-earth plasma.

Notice should also be taken of the results of investigations of the altitude dependence of the electron concentration in the outer ionosphere, obtained recently with the "Elektron" satellite in the altitude range Z ~ 2—20 thousand km [51]. In these experiments, the electron concentration was determined from satellite measurements of the electromagnetic radiation of outer space at frequency 1525 kHz. Owing to the influence of the ionospheric plasma on the radiation resistance of the receiving antenna, the level of the received cosmic radiation changes strongly when the satellite passes through the ionosphere. One can therefore calculate, taking into account the variation, of the equivalent capacitance of the antenna in the ionosphere, the electron concentration of the plasma along the orbit in the vicinity of the receiver mounted on the satellite. The results of these measurements are generally in good agreement with the N(Z) plots shown in Fig. 1. From data of [51] we get $N \simeq 10^4$ el/cm^3 at altitude Z ~ 2,000—3,000 km, decreasing smoothly to $N \sim 10^3$ el/cm^3 at Z ~ 10—15 thousand km.

A large amount of material on the outer ionosphere has recently been accumulated by analyzing the results of observations with the aid of the satellite "Alouette," on which a pulsed ionospheric station was mounted, probing the outer part of the ionosphere from the height of its principal maximum $N_{MAX}F^2$ to Z ~ 1,000 km. The results were published in a number of papers [52-56,58]. The general aggregate of these measurements shows that in the indicated region of altitudes, the altitude dependence of N(Z) is smooth and changes within limits that agree well with the data given in Fig. 1.

An analysis of all measurements of N(Z), shown in part in Fig. 1 (a large number of other measurement results were also considered) leads, in particular, to the recommendation that the average N(Z) plot shown in Fig. 7 be used in various calculations for the outer ionosphere. Above 15,000 km it is necessary to consider two possible variants of N(Z).

We have already noted that the altitude dependence of N(Z) contradicts curve 10, which was obtained with the aid of ion traps on the rocket "Luna 2" [10].

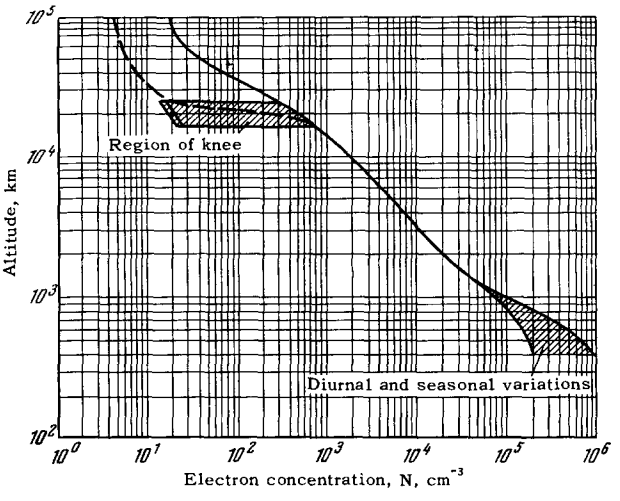

FIG. 7

Difficulties arise also in other investigations when attempts are made to determine the plasma concentration from the values of the currents. This can be seen, for example, on curves 21 of Fig. 2, which were registered with the aid of ion mass spectrometers on OGO-A [21].

Curve 10 diverges greatly from all the results of various other experiments in the altitude region of 1,000 km and above. Quantitatively the values of N(Z) recommended in [10] differ in the altitude region 1,000—2,000 km by a factor of 30—40. Even more striking are the sharp drop of N at Z ~ 1,000—1500 km and the subsequent constancy of N(Z) up to Z ~ 10—15 thousand km, which in general does not agree with the physical notions concerning the ionosphere. We note that here $H_0^2/8\pi$ is larger by 10^{12}—10^5 times than the energy density of the fluxes incident on earth, and is larger than $N\kappa T$ by approximately the same factor. When Z ~ 15—20 thousand km, the curve 10 of Fig. 1 has an additional bend and falls in the region of the knee. At the same time, this change in the variation of curve 10 of Fig. 1 has no bearing whatever on the previously-observed knee-like variation of N(Z) observed, which has been observed so far only with the aid of atmospherics. This can be

clearly seen in Fig. 2, where curve 10 is drawn to a linear altitude scale. It is seen there that when Z ~ 15—20 thousand km the rate of decrease of N(Z) (curve 10) slows down only slightly. On the other hand, the phenomenon of the knee is characterized by a rapid almost-jump-like change of the electron concentration only, as illustrated by curve 6.

Let us see now how curve 10, obtained by recalculating the measured values of the currents in ion traps, agrees with the altitude variation of the current, I(Z), registered with the aid of ion mass-spectrometers and shown by curves 21 on Fig. 2.[21] These curves are shown in Fig. 2 for atomic-hydrogen ions. Above 1,000—1200 km, however, as is well known by now, the protons are the principal component of the ionosphere[20]. In[21], the results of measurements for helium also show that it constitutes only several per cent of the composition of the external ionosphere. Therefore curves 21 actually characterize the general state of the plasma.

The measurement results represented by curve 21 correspond to different conditions of magnetic disturbance and represent the altitude variation of the current I(Z) in amperes (lower scale of Fig. 2). The authors of[21] exercise the required degree of caution and set the values of the current in correspondence with the values of the concentration (upper scale of Fig. 2) only tentatively. We see that above 1000 km curve 10, regarded as the altitude dependence of the current I(Z), does not contradict in general the altitude vs. current curves 21. Taken together, however, curves 21 and 10 not only do not agree, with the altitude variation of the concentration N(Z), but contradict it. This can be seen from the following:

In the altitude range 1—10 thousand km, I(Z) changes very slowly, and in some cases even decreases with decreasing altitude (two such curves 21 are shown in Fig. 2). This does not tie in at all with the normal variation of N(Z).

Second, the "saturation" of the I(Z) curves occurs in different experiments at greatly differing altitudes. In Fig. 1 these altitudes range from 13 to 28 thousand km, and go far beyond the region of the knee (see Fig. 1). Third, finally, if we assume for an instant that the values of N(Z) obtained from the I(Z) curves are correct, then we see that the concentration reaches unity in the region where they exhibit saturation, and continues to drop, which does not agree with the value of N(Z) in this region of altitudes. These values of N are approximately one-tenth of even the neutral-particle concentration, which should be close here to the minimum limit of N(Z). As we have already seen, when Z $\gtrsim$ 30,000 km the decrease of N(Z) does in general slow down appreciably, and the particle concentration tends almost to a constant value N ~ 5—10 el/cm^3.

Thus, the results of[10] and[20] do not give the correct altitude dependence of the particle concentration of the outer ionosphere, which on the average has already been sufficiently reliably investigated by now.

In connection with the foregoing, it is surprising that the authors of[10] have constructed the aforementioned model of the outer ionosphere on the basis of only one series of measurements, and have even stated that they were the first to establish the existence of hitherto unknown plasma sheath of the earth in the 2—20 thousand km altitude region[10].

2. EFFECTIVE TEMPERATURE AND OTHER PROPERTIES OF THE OUTER IONOSPHERE

The results of measurements of the temperature in the lower regions of the ionosphere and of the average energy of the low-energy "thermal" particles in the outer ionosphere and above it are shown in Fig. 8. To construct Fig. 8 we use the results of the papers cited earlier[12-14,17], and also other published data[27,28]. Unfortunately, at the present time the measurement results above 1,000 km are still quite scanty, and for the altitude region near 1—6 thousand km we found no suitable data at all.

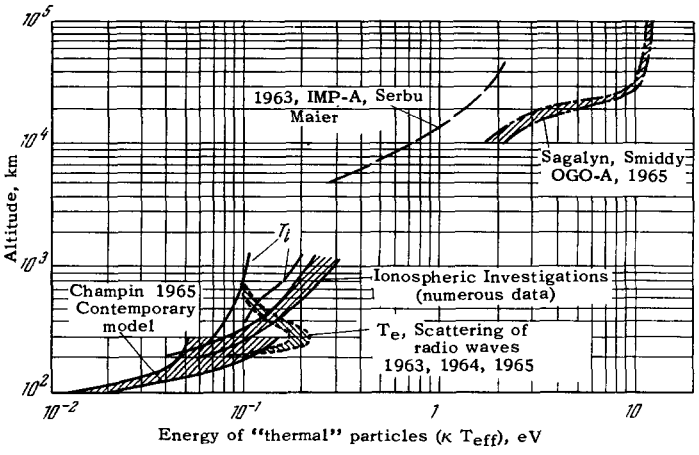

FIG. 8

Nonetheless, the general picture of the variation of the energy of the "thermal" particles with altitude can be outlined quite definitely.

Up to Z ~ 1,000 km, a very large amount of data has been accumulated. We cite only a few sources. Under different conditions, the temperature fluctuates in the range indicated in Fig. 8: for Z ~ 300—400 km, i.e., in the region of the principal maximum, κT_{eff} ~ 0.05—0.1 eV, and when Z ~ 1,000—1200 km we have κT_{eff} ~ 0.1—0.3 eV. One of the most important properties of this region of the outer ionosphere is that when Z ~ 200—700 km the ion temperature T_i is not equal to the electron temperature T_e. The ionosphere is not isothermal here, the maximum difference being observed at Z ~ 250—350 km; in

many cases T_e (3—4) T_i. These results were obtained from an analysis of the energy spectra of the radio waves "incoherently" scattered by the ionosphere [12,13]. The nonisothermal nature may be the consequence of the influence, of the electric field or, conversely, the cause of its appearance. On the other hand, we can assume that quasi-neutrality is violated: $N_e \neq N_i$. It is also natural to expect violation of the equilibrium Maxwellian distribution of the particle velocities in this region. We do not know, however, the results of experiments that can indicate these violations. For higher regions of the ionosphere (see below), however, such data are available.

The presence of "hot" accelerated electrons at Z ~ 200—700 km should contribute to the instability of the plasma and to the excitation of waves and oscillations in it—to cloud formation of the ionosphere. An investigation of this set of problems is of great interest (see Sec. 4).

Above 10,000 km, as can be seen from Fig. 8, the effective temperature increases rapidly from κT_{eff} ~ 1 eV to κT_{eff} ~ 10 eV at Z ~ 30,000 km.* When Z ~ 30—40 thousand km, the particle energy remains almost constant. It is interesting to note that such a variation of κT_{eff} is qualitatively in good agreement with the variation of the electron concentration (see Fig. 1). In the region of the knee, where fast changes of N(Z) take place and the plasma is nonstationary, there is also a rapid change in the particle energy. The data presented here for large altitudes were obtained principally for the analysis of the results of measurements carried out recently on OGO-A [17]. In the analysis of these data, attention must be called to one more very important circumstance.

In [17] are given the fluxes $(\overline{Nv})_i$ and concentrations N_i of the positive ions, and the electron fluxes $(\overline{Nv})_e$, at distances 20—160 thousand km from the earth. The values of κT_{eff} shown in Fig. 8 were obtained by us from the ratio $(\overline{Nv})_i/N_i$. There are much fewer measurement results for electrons. It can be noted, however, that $((\overline{Nv})_e/(\overline{Nv})_i)\sqrt{m/M} > 1$ for all the presented data. This ratio ranges from 1 to 2.6 and its average value is 1.6. We point out that in the limiting region of the outer ionosphere, at altitudes 20—30 thousand km, the range of this ratio is 1.3—1.6. Inasmuch as $v_i >> V_0$ (V_0 is the velocity of the satellite) everywhere in the considered altitude region, the foregoing inequality is evidence that the electron energy density exceeds the ion energy density. Their difference is

$$\Delta W \simeq (N\varkappa T)_e - (N\varkappa T)_i \sim 100 - 1000 \text{ eV}.$$

If we now assume for an instant that this is due entirely to the absence of quasi-neutrality $N_e \neq N_i$, and that $\Delta W \sim E_0^2/8\pi$, then we find that the electric field intensity is $E_0 \sim (1—4) \times 10^{-2}$ V/cm, i.e., the electric field is strong. The extent to which this important conclusion is correct will be demonstrated by future experiments. It should be noted that in general it agrees with the overall picture of the nonstationary state of the plasma at these altitudes, and also with the following results of investigations of the outer ionosphere:

At distances 12—25 thousand km from the earth, an analysis of the cutoff frequencies of the so-called nose whistlers (see Sec. 3) has yielded the differential energy spectrum of the electrons—the particle velocity distribution in the energy region 200—2000 eV [7]. Figure 9 shows the corresponding results, in the form of a plot of

$$\left(\frac{df}{dv}\right)_{v_Z=-v_0} = 2\pi \int_0^\infty f(v_r,\ v_Z = -v_0)\, v_r\, dv_r$$

against $E_u = Mv_0^2/2$, where $f(v_Z, v_r)$ is the distribution function in a cylindrical coordinate system (v_Z is directed along the magnetic field) and

$$\int_0^\infty dv_r \int_{-\infty}^{\infty} dv_Z f(v_r, v_Z) = 1.$$

This analysis method is discussed briefly in Sec. 3. It follows from Fig. 9 that

$$\left(\frac{df}{dv_Z}\right)_{v_Z=-v_0} \sim \frac{1}{v_0^2} \sim E_u^{-1}.$$

We note that for a Maxwellian velocity distribution

$$\left(\frac{df}{dv_Z}\right)_{v_Z=-v_0} \sim v_e^2 \exp\left(-\frac{v_0^2}{v_e^2}\right).$$

We see that the obtained data lead to a very important consequence, namely: the Maxwellian velocity distri-

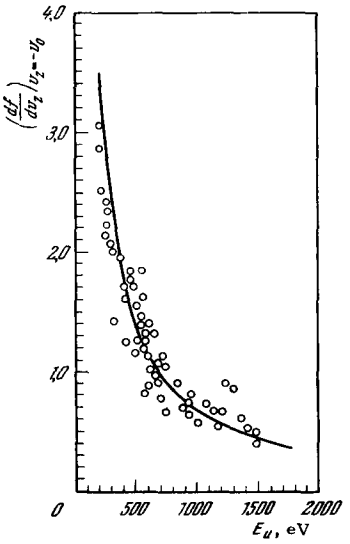

FIG. 9

*The data of [61] confirm that at Z ≈ 30 thousand km the temperature reaches not 10 eV, but about 2 eV (see [14] and Fig. 8) and changes little up to Z ≈ 100 thousand km. These data disagree with the results of [17].

bution is greatly violated at the limits of the outer ionosphere and higher. The distribution tail includes electrons of increased energy. The rise of the tail of the distribution (the acceleration of the electrons) is possible, and is due to the electric field indicated above. One can assume, naturally, that not the entire tail is raised, and that it has only an additional maximum or maxima in the indicated region of energies, due to various electron beams. Both cases, as is well known, contribute to an intensification of the plasma instability.

3. CONCERNING SOME METHODS OF INVESTIGATING THE OUTER IONOSPHERE

Let us examine briefly the theoretical methods for reducing the measurement results, with the aid of which, in particular, a number of the data used above were obtained. We shall note also certain shortcomings and difficulties of these methods.

A. Investigations with the Aid of Low-frequency Waves

This, in this author's opinion, is one of the most promising methods. An analysis of the character of propagation of low-frequency waves in the near-earth plasma reveals its main physical properties, and the method itself is closely related physically to the corresponding problem.

At the present time, when speaking of studies of the ionosphere with the aid of low frequency waves, one has primarily in mind investigations of whistlers. In plasma theory they are sometimes called holicons; they encompass the range of frequencies $\Omega_H \ll \omega < \omega_H$ and, in addition, their frequency satisfies the condition $\omega^2 \ll \omega_0^2/\omega_H$. It is known that these investigations are based on an analysis of oscillograms that register the dispersion of signals emitted by lighting discharges and propagating over long paths in the ionosphere. Namely, a study is made of the frequency dependence of the time of group delay of the wave spectrum of the signal

$$\tau(\omega) = \int_{(s)} \frac{ds}{U(s)} = \frac{1}{c}\int_{(s)} n_g\, ds$$

where U(s) is the group velocity, $n_g = n + \omega\, dn/d\omega$ is the so-called group coefficient of refraction, n is the refractive index, and ds is the path elements; the integral is taken along the wave-propagation trajectory. It is postulated that the trajectory coincides with the magnetic-field line, since whistlers are recorded at points situated on opposite ends of the magnetic force line that begins in the emission region of the lightning discharge—the source of the waves [4]. It must be noted, however, that the causes of the channeling of these waves along the magnetic-field line are insufficiently clear and call for further research, since waves of this type can easily propagate in a plasma in a large range of angles relative to the magnetic field. It can be assumed that such guiding of the whistler wave spectrum is enhanced by elongated ionized clouds situated along the magnetic field. The question of finding such inhomogeneous formations and investigating them up to the outermost border of the ionosphere is therefore of great interest.

Figure 10 shows groups of whistlers. These signals, which have two branches, are called nose whistlers, and the frequencies $\omega_N/2\pi$ at which the delay times have a minimum, are called nose frequencies. The range of frequencies of the whistlers, shown in Fig. 10, corresponds to a part of the wave spectrum emitted by the lightning discharge, and varies in different experiments in the range $\omega/2T \sim 1$—10 kHz. The propagation of waves of this type in a plasma is determined principally by the motion of the electrons. Therefore waves with right-hand polarization, corresponding to the extraordinary wave, are not strongly damped.

However, the spectrum of the signals radiated by lightning discharges, is much broader than the indicated frequency range. Near the earth, the spectrum of the whistlers ranges from a few to several dozen kHz [29]. On the other hand, the low-frequency waves, down to several Hz, pass freely in the outer ionosphere [30]. Besides, it is well known that at frequencies lower than the gyrofrequency Ω_H of the ions in the plasma, two waves can propagate. One is the already mentioned extraordinary wave, which is a fast magnetosonic wave when $\omega \ll \Omega_H$. The other wave, the propagation of which is determined by the motion of the ions, has right-hand polarization (ordi-

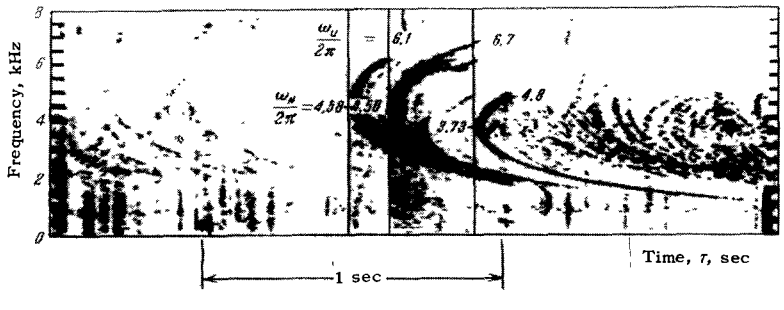

FIG. 10

nary wave), and is produced as an ion cyclotron wave, which is an Alfven wave at frequencies $\omega \ll \Omega_H$.

An important problem was therefore the analysis of the nature of the frequency cutoff of this type of whistler, and also a search for corresponding signals down to the range of several Hz.

Recently, in satellite experiments in the ionosphere, both indicated waves were observed in the infralow frequency range from 100 to 500—600 Hz[31-34], the source of which are lightning discharges. These waves were called respectively "electron" and "ion" (proton) whistles (Fig. 11). The first is the "tail" of an ordinary infralow-frequency whistler which has, however, covered only a short path from the source to the satellite, while the second is an ion-cyclotron wave, cut off at the gyrofrequency of the ions and covering the same path.

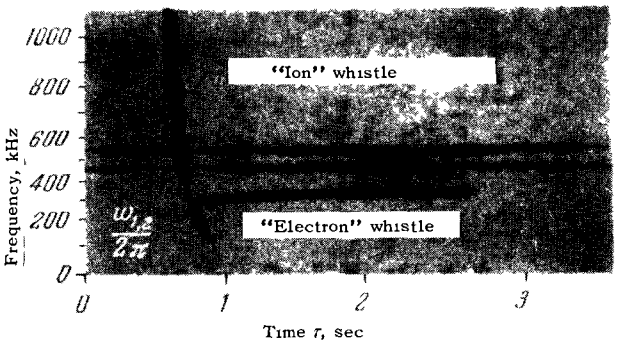

FIG. 11

The physical gist of the analysis method used for whistlers of both types, and the information on the structure of the outer ionosphere obtainable from this analysis, consist in the following.

From the dispersion curves of the ordinary signals one determines first the electron concentration at the apogee of the wave trajectory, from the nose frequency ω_N and from the delay time τ_N. This is done by comparing the corresponding values of ω_N and τ_N with the results of calculations of a family of $\tau(\omega)$ curves. The analytic $N(Z)$ dependence is used in the calculations. The functions most frequently used are

$$N(Z) \sim C_0 \left(\frac{R_0}{R}\right)^3, \quad N(Z) \sim C_0 \left(\frac{R_0}{R}\right)^3 \exp\left(\frac{R_0}{R}\right),$$

where R_0 is the radius of the earth and R is the distance from its center. These functions, with a suitable choice of constants, are in general good agreement with the $N(Z)$ plots shown in Fig. 7 for $R \sim (1—6)R_0$. Of course, they differ in the region of the knee, where $N(Z)$ falls off rapidly. It is therefore important to use subsequently a theoretical family of $\tau(\omega)$ curves calculated for this $N(Z)$ dependence, and to verify the extent to which this affects the electron density determined from the experimental data. Such a check apparently necessitates a noticeable correction in the values of N for the cases when a knee is observed. Since usual atmospherics (see Fig. 10) are registered at frequencies which much greatly exceed the ion gyrofrequency Ω_H, we can neglect the influence of the ions in the expression for the refractive index. In many cases, however, it is necessary to take into account the influence of the thermal motion of the electrons—the kinetic correction to the refractive index. As a net result, in the realizable case when $\omega_0^2 \gg \omega\omega_H$, we get for longitudinal wave propagation

$$n = \frac{\omega_0}{\sqrt{(\omega_H - \omega)\omega}}\left[1 + \frac{1}{2}\left(\frac{v_e}{c}\right)^2 \frac{\omega_0^2\omega}{2(\omega_H - \omega)^3}\right], \tag{2}$$

$$n_g = \frac{1}{2}\frac{\omega_H\omega}{\sqrt{\omega(\omega_H - \omega)^3}} + \frac{1}{2}\left(\frac{v_e}{c}\right)^2 \frac{\omega_0^2\sqrt{\omega}\left(\frac{3}{2}(\omega_H + \omega)\right)}{2\sqrt{(\omega_H - \omega)^9}}, \tag{3}$$

where $v_e = \sqrt{2\kappa T/m}$ is the thermal velocity of the electrons, ω_H and ω_0 are the gyro and Larmor frequencies, and c is the velocity of light. In spite of the smallness of the thermal corrections to n and n_g, they make noticeable contributions to the integrals. Therefore an analysis of the dispersion at two points of the atmospheric—at the nose frequency ω_N and the upper cutoff frequency ω_u of the atmospheric (see Fig. 10), reveals the influence of the thermal motion of the electrons and makes it possible to determine not only N but also the effective temperature at the crest of the wave trajectory[8].

An important question in the analysis of an ordinary whistler (see Fig. 10) is: what determines the frequencies at which the signals are observed? Cutoff at the minimal frequencies $\omega/2\pi \sim 1$ kHz has not been analyzed theoretically to this day. It is not excluded that a suitable reduction of the measurement results may be fruitful. On the other hand an analysis of the cutoff frequencies $\omega_u/2\pi \sim 8—10$ kHz at the upper limit of the whistlers had led to very important results[7]. This cutoff is due to thermal motion of the electrons and corresponds to cyclotron-resonance damping at the electron gyrofrequency ω_H. Since the damping occurs at the crest of the wave trajectory, i.e., in a relatively narrow region of the ionosphere, the corresponding analysis of the whistlers is a very sensitive method of determining the wave damping coefficient itself.

As is well known, cyclotron gyroresonant absorption of the wave occurs when the velocities v_Z of the electrons along the magnetic field satisfy the condition

$$-v_Z = v_0 = \frac{\omega_H - \omega}{\omega}\frac{c}{n}, \tag{4}$$

i.e., when the Doppler shift of the frequency "seen" by the electron is equal to $\omega(v_0/c)n$. The wave damping coefficient is here

$$\varkappa = \frac{\pi}{2} c \frac{\omega_H - \omega}{\omega}\left(\frac{df}{dv_Z}\right)_{v_Z = v_0}. \tag{5}$$

where f is the distribution function and

$$\left(\frac{df}{dv_Z}\right)_{v_Z=-v_0} = 2\pi \int_0^\infty f(v_Z,\ v_Z = -v_0)\, v_r\, dv_r \qquad (6)$$

is the differential energy spectrum of the electrons, since $N(df/dv_Z)_{vZ=-v_0}$ is the number of particles having a velocity $v_Z = -v_0$. The energy-spectrum results presented in Sec. 2 (see Fig. 9) were obtained from the value of κ calculated from the cutoff frequencies ω_u.

Let us consider now a method for analyzing the infralow-frequency signal oscillograms shown in Fig. 11. The refractive indices of both waves, for $\omega \ll \omega_H$ and $\omega_0^2 \gg \omega\omega_H$ are respectively:

$$n_1^2 = \frac{\omega_0^2}{\omega\omega_H} - \frac{\Omega_{01}^2}{\omega(\Omega_{H1}+\omega)} - \frac{\Omega_{02}^2}{\omega(\Omega_{H2}+\omega)} - \ldots, \qquad (7)$$

$$n_2^2 = -\frac{\omega_0^2}{\omega\omega_H} + \frac{\Omega_{01}^2}{\omega(\Omega_{H1}-\omega)} + \frac{\Omega_{02}^2}{\omega(\Omega_{H2}-\omega)} \quad \ldots, \qquad (8)$$

where $\Omega_{01}^2, \Omega_{02}^2, \ldots, \Omega_{H1}, \Omega_{H2}, \ldots$ are the Larmor and gyrofrequencies of the ions of the different sorts, and $N_1, N_2, \ldots$, and $M_1, M_2, \ldots$ are their densities and masses (N—electron density). Formulas (7) and (8) were written without allowance for thermal corrections and for the number of collisions. In taking the number of collisions into account, it is necessary to add everywhere to the mass symbols m, M_1, $M_2, \ldots$ the factor $1 + i\nu/\omega$, where ν is the collision frequency of particles of sort i.

Formula (7) is equivalent to formula (2) with $\omega \ll \omega_H$, and makes due allowance for the ions. It corresponds to an electron wave whose refractive index is larger than zero everywhere. On the other hand, the refractive index n_0^2 of the second wave—ion wave—is larger than zero only in discrete frequency regions. Putting for convenience $\Omega_{H1} > \Omega_{H2} > \ldots$, we see that the first region $n_0^2 > 0$ begins at $\omega = \Omega_{H1}$ and extends to the value of ω at which the refractive index n_0^2 has the first zero ($n_2 = 0$); when ω_1 decreases further, n_2^2 again becomes negative. Then n_2^2 becomes positive in a second region at $\omega \lesssim \Omega_{H2}$, etc. At the points $\omega \sim \Omega_H$ we have $n_2^2 \to \infty$, i.e., the wave velocity decreases rapidly here and the wave delay time increases rapidly. This explains the steep growth and then practically horizontal section of the dispersion curve in Fig. 11 for the ion signal. The dispersion curve in Fig. 11 corresponds to the frequency of ions having the least mass—protons. We see that ion whistlers determine the gyrofrequencies of the ions, and if the magnetic field is known they determine the composition of the ionosphere. Further, a very important feature of these oscillograms is the point of intersection of the two dispersion curves, where $n_1^2 = n_2^2$. In Fig. 11 the corresponding value of the frequency at this point is denoted $\omega_{1,2}$. This frequency determines the ratio N_1/N. Thus, for example, if we take into account only the influence of ions of one sort, we can obtain from (7) and (8)

$$\omega_{1,2} \simeq \Omega_{H1}\sqrt{1 - \frac{N_1}{N}}. \qquad (9)$$

Thus, an analysis of ion whistlers gives very extensive information on the properties of the outer ionosphere. Interest attaches to further research at even lower frequencies than shown in Fig. 11. Naturally, the registration of such signals at different altitudes will yield the corresponding altitude variation of the indicated quantities.

In concluding this section, we note that we have considered here only questions connected with "passive" electromagnetic waves, whose source lies outside the plasma. Yet intrinsic excitation of the ionospheric plasma itself at low frequencies is also possible (and has already been observed in many cases) [35-38]. So far, such radiation has been observed at frequencies from several hundred to several thousand Hz. It is important, however, to search for corresponding "active" waves and plasma oscillations at frequencies near the ion gyrofrequencies, down to several Hz, directly in the plasma (using satellites or rockets). Besides the large information on the structure and parameters of the ionosphere which such research can yield, it also reveals the mechanisms of its statistical inhomogeneities and cloud formation, and permits a study of the instabilities and of other important properties of the ionosphere.

B. Investigations of "Incoherent" Radio-wave Scattering

Measurements of the intensity and of the spectra of the radio waves scattered by the plasma enable us to study various properties of the ionosphere. Physically, this method is based on the interaction of the radio waves with the plasma. Therefore, the results of the corresponding measurements provide a thorough diagnosis of the plasma. The scattering of radio waves in the ionosphere [40] was observed soon after the publication of the very first paper in which the possibility of such research was indicated [39], and by now this method yielded many results, some of which were reported above [11-13].

The measurement of "incoherent" scattering of radio waves consists mainly of radiating vertically upward short packets of high-intensity radio waves of frequencies greatly exceeding the maximum plasma frequency of the ionosphere

$$\omega_{0,\max}^2 = \frac{4\pi(N_m F2)\, e^2}{m}.$$

The delayed back scattering of this packet of waves from different heights of the ionosphere Z is recorded. One of the first such oscillograms is shown in Fig. 12 [40]; it contains the record of the continuous field of "reflected" signals from different heights of the ionosphere. Integration of the intensity of the scattered waves in individual altitude sections $\Delta Z = c\Delta t$, effected directly with the aid of integrators at the output of the receiver, results in oscillograms of the type shown in Fig. 13. On the oscillogram, the

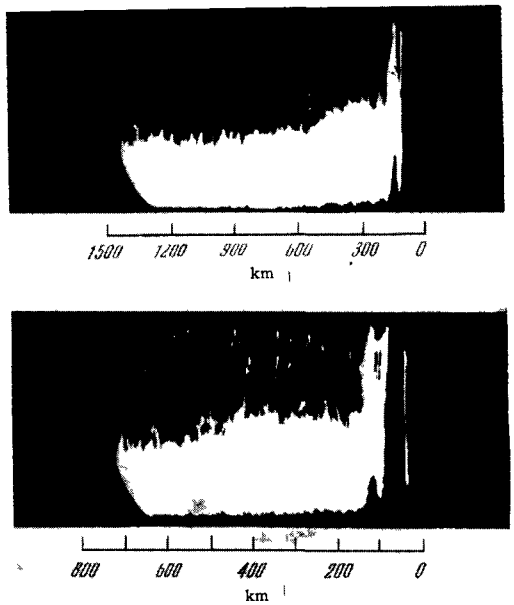

FIG. 12

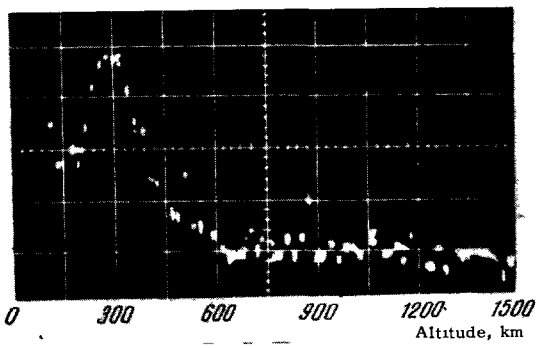

FIG. 13

vertical deflection of the point is already proportional to the intensity of the scattered waves in the interval (Z + ΔZ), so that such an oscillogram gives directly the altitude variation of the scattering energy. We note that in one of the best setups for "incoherent" radio wave scattering, operating at 50 MHz, the signal pulse power was $\sim 5 \times 10^6$ W, the antenna area was $8\,4 \times 10^4$ m^2, and the pulse width was $\sim 3 \times 10^{-3}$–10^{-4} sec. The apparatus radiated alternately, at fixed time intervals τ, waves circularly polarized in opposite directions [12]. This has made it possible to determine the phase difference between the ordinary and extraordinary waves, and also the temporal autocorrelation function, which is proportional to the Fourier-transformed energy spectrum.

Let us examine the physical principle of the method and its possibilities, bearing in mind that the frequency of the incident wave is $\omega \gg \omega_{0,\max}$. The radio waves are scattered in the plasma by spontaneous "thermal" fluctuations of the electron density $\delta N(\omega)$. With this, inasmuch as a self-consistent Coulomb interaction exists in the plasma between the electrons and the ions, $\delta N(\omega)$ depends on the ion motion. Therefore the scattering of radio waves in the ionosphere can in general not be a purely coherent scattering of the Thomson type by free electrons. When the incident wave interacts with the plasma, the collective properties of the plasma come into play. The more the wavelength of the incident radiation $\lambda = 2\pi c/\omega$ exceeds the Debye wavelength

$$D = \sqrt{\frac{\varkappa T}{4\pi \Lambda e^2}} \simeq \frac{v_e}{\omega_0},$$

i.e., when the condition

$$\frac{\lambda}{2\pi D} > 1 \tag{10}$$

is satisfied, the greater the influence of the ions. Thus, purely incoherent Thomson scattering takes place only if

$$\frac{\lambda}{2\pi D} \ll 1. \tag{11}$$

In this latter case the differential scattering cross section, i.e., the spectrum of the Doppler frequency shifts

$$\Omega_s = \omega_s - \omega - kv_e = \frac{\omega}{c} v_e \tag{12}$$

of the scattered waves, has a Gaussian character, owing to the Maxwellian distribution of the electron velocities. The spectrum is bread and its width is of the order of $kv_e = k\sqrt{2\chi T/m}$. Indeed, it is easy to see that the frequency distribution of the back scattering per unit volume in a unit solid angle is equal to

$$\sigma_{\Omega_s}\, d\Omega_s = N f_0(v)\, dv \cdot \frac{\sigma_e}{4\pi}, \tag{13}$$

where N is the electron density,

$$f_0(v) = \frac{1}{\sqrt{\pi} v_e} \exp\left(-\frac{v^2}{v_e^2}\right)$$

is the Maxwellian distribution and

$$\sigma_e = 4\pi \left(\frac{e^2}{mc^2}\right)^2$$

is the isotropic electron scattering cross section. Using (12) we find that the scattering cross section per unit solid angle is

$$\sigma_{\Omega_s}\, d\Omega_s = \frac{N\sigma_e}{4\pi} \frac{1}{\sqrt{\pi} k v_e} \exp\left(-\frac{\Omega_s^2}{(kv_e)^2}\right) d\Omega_s, \tag{14}$$

and the total scattering cross section over all frequencies and angles is

$$\sigma = 4\pi \int \sigma_{\Omega_s}\, d\Omega_s = N_0 \sigma_e, \tag{15}$$

i.e., it coincides with Thomson's formula. In this case the radio waves are scattered not by the electron-density fluctuations but by the electrons themselves.

For an arbitrary value of $\lambda/2\pi D$, i.e., when Debye screening of the electron by the ions is in effect, the formulas for $\sigma_{\Omega S}$ are much more complicated. An analysis of the calculation results shows that the scattered radiation presents a highly harmonic physical picture.[41-43]

For an arbitrary value of $\lambda/2\pi D$, the total cross section of the back scattering per unit solid angle in an isothermal plasma is

$$\sigma = \frac{N\sigma_e}{4\pi} \frac{1}{2+\left(\frac{2\pi D}{\lambda}\right)^2}, \quad (16)$$

from which we see that when $\lambda/2\pi D \gg 1$ we have

$$\sigma = \frac{1}{4\pi} \frac{N\sigma_e}{2}. \quad (17)$$

Thus, owing to the action of the ions, the total scattering energy at all frequencies is reduced by one-half when $\lambda \gg D$. On the other hand, the scattering-energy frequency distribution has a number of singularities.

For an isothermal plasma ($T_e \sim T_i$), assuming first that there is no external magnetic field, the scattering spectrum consists of two parts. The greatest part of the scattering energy lies in the frequency region $\Omega_s \sim kv_i$. This is the Doppler-broadened fundamental line of the spectrum—its ionic part. In the electronic part of the spectrum, at frequencies $\Omega_s \sim kv_e$, the scattering intensity is much smaller throughout. When $\lambda/2\pi D \sim 1$, satellites begin to appear in the electronic part of the spectrum—maxima which become quite narrow when $\lambda/2\pi D \gg 1$ and correspond to the electron Langmuir frequency, i.e., in this case $\Omega_s \sim \omega_0$. The reason is that the fluctuations of the electron concentration in this case occur on longitudinal electron oscillations. It is seen from Fig. 14 that Ω_s is already sufficiently close to ω_0 even when $\lambda/2\pi D = 4$. Indeed, for $\lambda/2\pi D = 4$ we have

$$\Omega_s = 3.5\, kv_e \sim 3.5 \frac{2\pi D}{\lambda} \cdot \omega_0 \sim \omega_0.$$

In an isothermal plasma, the character of the scattering spectrum changes noticeably.

When $T_e \gg T_i$, the fluctuations of the electron concentration occur already on longitudinal ion-sound waves $\omega = kV_s$, where $V_s = v_i\sqrt{T_e/T_i}$ is the velocity of non-isothermal sound. Consequently maxima at frequencies $\Omega_s = kv_i\sqrt{T_e/T_i}$ appear in the spectrum. It is easy to see from Fig. 4 that the role of the ion-sound wave becomes noticeable already at $T_e/T_i \sim 2$. This result of the theoretical calculations of the scattering spectra is in itself quite interesting. In a non-isothermal plasma with $\lambda/2\pi D \gg 1$, the total differential cross section per unit solid angle is equal to

$$\sigma = \frac{N_0\sigma_e}{4\pi} \frac{1}{1+\frac{T_e}{T_i}}. \quad (18)$$

The magnetic field $\mathbf{H}_0$, as is well known, leads to an increase in the number of oscillation modes and waves in the plasma, and this, of course, should become manifest in the properties of the scattered radiation. The magnetic field, however, does not influence the scattering radiation when the direction of its wave vector k_s coincides with $\mathbf{H}_0$, and becomes noticeable only when $k_s \perp \mathbf{H}_0$.

We point out first that the properties of the total differential scattering cross section in a magnetic field remain the same as in an isothermal plasma, and are described with the aid of (16). On the other hand, the spectral distribution acquires the following peculiarities.

Just as in the case when $\mathbf{H}_0 = 0$, the high frequency fluctuations of the electron density $\delta N(\omega)$ occur on Langmuir plasma oscillations if $\omega \gg \omega_0$, i.e., on high-frequency longitudinal waves. Therefore the scattering spectrum has a maximum for $\lambda/2\pi D \gg 1$ at the hybrid frequencies

$$\Omega_s^2 = \omega_{1,2}^2 = \frac{1}{2}(\omega_H^2 - \omega_0^2) \pm \frac{1}{2}\sqrt{(\omega_H^2+\omega_0^2)^2 - 4\omega_H^2\omega_0^2\cos^2\theta} \quad (19)$$

in the electronic part of the spectrum ($\Omega_s \sim kv_e$).

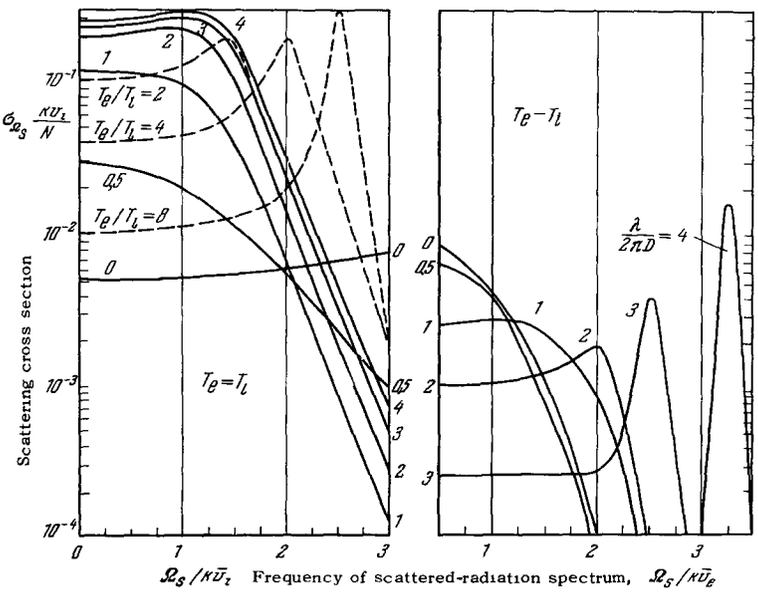

FIG. 14.

In the low-frequency part of the spectrum, when $\Omega_S \sim kv_i$, the spectrum is an isothermal plasma with $k_S \perp H_0$ should have a maximum at the frequency of the fast magnetosonic wave, i.e., when

$$\Omega_s = kV_A, \tag{20}$$

where $V_A = \Omega_0/\Omega_H$ is the Alfven velocity (Ω_0 is the ion Langmuir frequency). In a strongly nonisothermal plasma, when $T_e \gg T_i$, scattering by slow magnetosonic waves also occurs, and the spectrum should have additional maxima at

$$\Omega_s = kV_s. \tag{21}$$

Naturally, side bands appear at the ion gyrofrequencies Ω_H corresponding to the frequencies of the ion-cyclotron waves. Scattering by Alfven fluctuations of the plasma ($\omega \ll \Omega_H$) should similarly appear in the spectrum.

The properties of the scattered radiation, which we considered briefly above, pertain to a two-component plasma. In a multi-component plasma the ionic part of the spectrum is modified, and this part broadens when the light particles begin to predominate (for example, when $N_i(H_1) \ll N_i(0)$).

We see that a sufficiently complete theoretical analysis of the recorded scattered radiation of the ionosphere can yield much information on different plasma parameters. A feature of this method is that it depends in organic fashion on the vibrational properties of the plasma; by the same token, a sufficiently detailed analysis of the scattering spectra can also serve as an appropriate research tool. In particular, one must bear in mind observation of deviations from Maxwellian distribution.

A direct determination of the ratio of the total scattered-radiation intensity registered by the receiving unit to the incident-radiation intensity gives the total differential effective cross section per unit solid angle. We see that this cross section depends on the concentration N and on the ratio T_e/T_i. If T_e/T_i is sufficiently large, then the cross section can be determined from the maxima of the spectrum. However, the picture becomes more complicated in a multicomponent plasma. It is therefore necessary to determine N independently, say by measuring the phase difference ψ between the extraordinary and ordinary waves in a specified altitude interval. If the corresponding theoretical curves are used, the spectrum of the scattered radiation determines also the relative contents of the different plasma components. This is done by measuring the autocorrelation function

$$E(t)\,E^*(t+\tau)\sin\psi, \qquad E(t)\,E^*(t+\tau)\cos\psi.$$

The Fourier transform of $E(t)E^*(t+\tau)$ gives the energy spectrum of the scattering.

In conclusion it must be noted that the entire potential of the method of "incoherent" scattering has not yet been exhausted. A deeper insight into the theoretical methods of analyzing the measurement results can be gained by using electronic computers directly in the experiments. It is advantageous to effect at a single point simultaneous measurements at several frequencies, chosen such as to go through the values $2\pi D/\lambda \gg 1$, ~ 1, and $\ll 1$ in different regions of the ionosphere. Experiments with very narrow beams are important. These reveal, in particular, the influence of the magnetic field on the scattered-radiation spectra.

C. Investigations with the Aid of Langmuir-type Probes

The method of determining the concentration of charged particles and other parameters of the ionosphere from measurements of a particle flux drawn from the surrounding medium into chambers of various constructions (mass spectrometer, ion traps, spherical analyzers) is based on the principle of the Langmuir probe, which was developed more than 40 years ago [44]. It was first used for the ionosphere in 1946 [45]. The Langmuir probe, generally speaking, is an elegant and fruitful means of investigating the properties of a highly rarefied plasma. However, when used under the conditions of interest to us, it is subject to a number of limitations and requires great caution.

In different regions of the near-earth plasma, noticeable changes occur in the characteristic parameters of the medium (particle velocity, Debye radius, Larmor radii, potential of the body, etc.), and a corresponding change takes place in the effects produced in the vicinity of a moving body by its interaction with the plasma. It is frequently difficult in general to determine under what conditions the measurements were made, for example, if the potential φ_0 of the body is unknown. At the same time, exact knowledge φ_0 may be decisive for a correct utilization of the results of the measurements with the aid of probes. On the other hand, no sufficiently complete theory of probes, with allowance for various conditions of the external ionosphere (for example, with allowance for the magnetic field), has yet been developed. Consequently in many cases we do not know in general how to convert the measured value of I (current in the probe collector) into the sought density of the unperturbed medium. This explains, for example, why an incorrect altitude variation of the particle density was obtained from the measurements of the altitude variation of $I(V)$ (Sec. 1). We shall consider here briefly, by way of illustration, only a few peculiarities of probe measurements of the ion density in the ionosphere. Naturally, a complete analysis of this problem goes beyond the framework of the present article.

When the probe is moved a large distance from the

earth's surface, as is the case for example in the experiments described in [1] and [21], radical changes occur in the physical conditions under which the measurements are made. Therefore the theoretical relation that describes the connection between the concentration of the ions and the current I measured by the instrument changes in a complicated manner. At the present time, under certain conditions, it is not known at all what formulas can be used for this purpose. For concreteness let us consider the conditions at four fixed distances from the earth's surface, for which the main parameters determining I are given in the following table:

Altitude Z, km	$v_i = \sqrt{\frac{2\varkappa T}{M}}$	Velocity of space rocket, V_0	$\frac{V_0}{v_i}$	D, см	ρ_{He} cm	ρ_{H^+}, cm
500	10^5	10^6	10	0 6	4	$7\cdot10^2$
2000	$7\cdot10^5$	10^6	1 4	2 7	8	$3\cdot10^2$
6000	10^6	$8\ 10^5$	0.8	7.4	24	$1\cdot10^3$
20 000	$3\cdot10^6$	$5\cdot10^5$	0.16	10^2	$1.5\cdot10^3$	$3\cdot10^4$

It follows directly from the table, first, that already at Z ~ 2000 km it can no longer be assumed that the probe moves with supersonic velocity, for the particle velocities become commensurate here with the velocity of the body. Therefore when Z ~ 2000 km the formula

$$I = SeN_iV_0, \tag{22}$$

which is frequently used when $V_0/v_i \gg 1$, is no longer valid (S is the effective area of the instrument).

At lower altitudes, where V_0/v_i, formula (22) is in general suitable, but only ahead of the moving body, if the surface of the probe collides head-on with an incoming particle stream. On the other hand, a rarefaction region is produced in the rear of the body. For example, along its axis, at a distance $0.1\rho_0$ from the body (ρ_0 is the radius of the body), the particle density is approximately 1/10th of the unperturbed density N_0 of the plasma surrounding the body, with N depending strongly on the angle θ between the probe and the direction of motion of the body [46-48]. Therefore any accurate determination of the particle density calls for knowledge of the orientation of the probe relative to the vector V_0 and of the corresponding angle function. The latter, however, depends on many factors, in particular on the shape of the body and the distribution of its potential $\varphi_0(\theta)$. For certain potentials, a condensation region may even appear behind the body, in the vicinity of its motion axis, while to the side of the axis there is a rarefaction region. At the same time, not only is the potential of the body during the time of the measurements unknown, but there are even no sufficiently accurate methods for its determination. Since the body carrying the probe has a complicated geometrical and electric structure—its surface consists of conducting parts, dielectrics, and semiconductors—the distribution of its surface potential $\varphi_0(\theta)$ may be complicated. It is therefore not excluded that locally φ_0 can reach large values. This will greatly influence the characteristics of a probe placed near such a region. It is seen from the foregoing that the use of probe measurements to determine the concentration is quite difficult even in the regions where $V_0/v_i \gg 1$.

Let us consider now the higher altitudes. From Z ~ 2000 km up to Z ~ 6000 km we have $V_0 \sim v_i$. Furthermore, the Debye radius becomes commensurate here with the linear dimension of the probe (of the order of several centimeters). Under these conditions formula (22) is not suitable at all for the determination of the particle density, No other rigorous theoretical formulas, are available to functionally relate I with N_0. Furthermore, the influence of the magnetic field on the probe characteristics is expecially strong in this region. The electron Larmor radii become commensurate here with the probe dimensions, and then with the dimensions of the body. Under these conditions the particle flux captured by the probe can greatly decrease. The particles can "slip by" the probe. However, there is still no appropriate probe theory in which account is taken of the influence of the magnetic field.

At distances Z > 20,000 km from the earth, the Debye radius already exceeds the probe dimensions by several times ten. Moreover, for attracted particles (positive ions if the body potential is negative), the probe can be assumed to be at ($v_i \gg v_0$), and we can use the well known Langmuir formula

$$j \simeq Se\frac{Nv_i}{2\sqrt{\pi}}\left(1+\frac{e\varphi_0}{\varkappa T}\right) = j_0\left(1+\frac{e\varphi_0}{\varkappa T}\right). \tag{23}$$

However, formula (23) is valid in practice only if $(\varkappa T/e\varphi_0)\,(D/\rho_0)^8 \gg 1$ (see [44]). With increasing potential, the flux increases rapidly, namely:

$$j = j_0\left[\frac{|e\varphi_0|}{\varkappa T}\left(\frac{D}{\rho_0}\right)^{\frac{4}{3}}\right]^{\frac{6}{7}},$$

and conditions under which $j/j_0 \sim 20$ become possible even in this region of altitudes. Consequently, a particle density smaller by a factor of 20 produces in the instrument the same current as in the case when j is determined by formula (23). Yet the latter formula has been used to process the experimental data without taking into account the concrete measurement conditions.

Thus, the present-day theory used to reduce probe-measurement results does not permit a reliable investigation of the outer ionosphere with the aid of these methods; we emphasize that this is particularly true if

$$\frac{V_0}{v_i} \lesssim 1, \quad \frac{D}{\rho_0} \gtrsim 1, \quad \frac{\rho_{H_e}}{\rho_0} \sim 1, \tag{24}$$

i.e., in the altitude region from Z ~ 1500—2000 km to Z ~ 10,000—20,000 km. At large distances from the earth, Z > 20,000—30,000 km, the thermal energy of the particles is already sufficiently large (κT_{eff} ~ 10 eV), and consequently $e\varphi_0/\kappa T$ can hardly be very large. Further, the influence of the magnetic field should also be greatly reduced, since ρ_{H_e}, and certainly ρ_{H_i}, is much larger than the dimensions of the body, so that the trajectories of the particles relative to the probe can be regarded as straight lines. Furthermore, D is either larger or much larger than ρ_0 throughout. The net result is that the flux density is determined, as in a medium at rest, with the aid of formula (23), and the difficulties involved in using probes are greatly reduced. It should be noted that in many cases, even in the near-earth plasma zone in which probes are the least reliable, the conditions can be made favorable by choosing the proper shape of the body, by appropriate placement of the probe relative to the least-charged part of the surface, etc. Such measurement conditions, however, are difficult to foresee. Thus, further improvement of the quality of probe measurements is possible only if an adequate theory is developed for these measurements. With this, to obtain the full value the measurement results it is necessary in many cases to derive theoretical formulas for specified concrete experimental conditions, with due allowance for the dimensions and shape of the body, the placement of the probe relative to the body, the electric configuration and the reflecting properties (degree of accommodation) of its surface, etc.

4. INHOMOGENEOUS FORMATIONS IN THE OUTER IONOSPHERE

As is well known, the ionosphere is a statistically inhomogeneous medium, in which the inhomogeneous formations are created and annihilated almost continuously. Therefore the character of the ionosphere inhomogeneity is described with the aid of the spectra of the sizes of the inhomogeneous formations, the spectra of the fluctuations of their electron densities, the autocorrelation function of the scattered radiation, etc.[49,50]. The dimensions of the inhomogeneous formations range from hundreds of meters to hundreds of kilometers. The relative fluctuations of the electron density

$$\delta N = \frac{\Delta N}{N_0}$$

range from 10^{-3}—10^{-2} to several units. At the same time, naturally, inhomogeneous formations that vary "slowly," and are not describable statistically, are also observed in the ionosphere. These constitute principally the large-scale inhomogeneity of the ionosphere, which is described by a functional dependence on the time and the coordinates.

The statistical inhomogeneity of the ionosphere is closely related to the vibrational and wave properties of the plasma and to its interaction with the particle fluxes and the radiation incident on it. The occurrence of a local uncompensated charge, the action of the external electric fields, or the violation of the equilibrium distribution or of the isothermal conditions all lead to instability of the plasma and to various types of wave motions. Since the main physical parameters of the ionosphere (density, temperature, mean free path, Larmor radius) depend on the height and on the horizontal coordinates, the processes become more complicated. In general, a continuum of oscillations can exist in the entire ionosphere at a given instant of time. Moreover, just as in the ionosphere, drifts and general large-scale motions of the particles are observed, vibrational processes can develop, and turbulization of the plasma can set in.

We see that an investigation of the general physical characteristics and properties of the inhomogeneity of the ionosphere, particularly the outer ionosphere, is of great interest. It is important here also to investigate the shape of the inhomogeneities, the character of their orientation along the magnetic field, and the degree of their ellipticity. The degree of ellipticity observed in the lower region of the ionosphere is of order 2—4, i.e., relatively weakly elongated inhomogeneities. At the same time, we can assume that at large altitudes there exist inhomogeneous formations of "sausage" type, very strongly elongated along the magnetic field, since transverse diffusion in a weak-collision plasma is much slower than longitudinal diffusion. In particular, observation of such inhomogeneities would help explain the propagation of whistlers over long distances.

The altitude variations of the properties of the inhomogeneities thus reveal the character of the processes that occur in the ionosphere, and determine

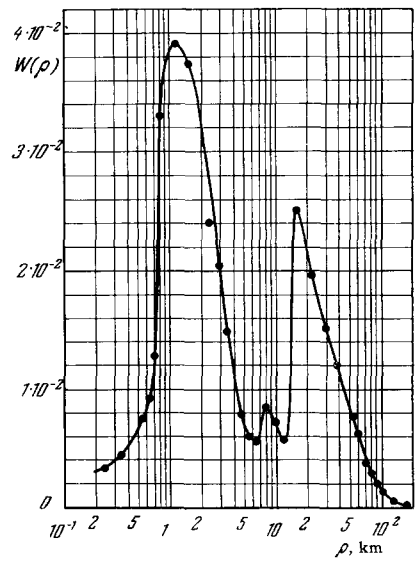

FIG. 15

its principal parameters. A very important experimental problem is to measure simultaneously, in local regions of the ionosphere, the dimensions of the fluctuations of the concentration of inhomogeneous formations and the plasma-oscillation frequencies. The author knows of no such experiments. They would establish, in particular, the type of the waves excited in the plasma and permit a thorough diagnosis of the plasma. We see that an investigation of the inhomogeneous structure of the ionosphere and of the plasma-wave processes connected with it is a fundamental problem. While noting these circumstances, we are unable, however, to construct at present any ordered picture of the corresponding data, especially in the outer ionosphere, owing to the scarcity and sporadic nature of the individual experimental results.

The latest investigations in the altitude region 400—2500 km with the "Elektron" satellite, using coherent radio waves, have made it possible to construct the spectra of the sizes of the inhomogeneous formations, $W(\rho)$, and of the fluctuation of their electron density, $W(\Delta N)$, by analyzing the fluctuations of the differences in the Doppler frequency shifts. These are shown in Figs. 15 and 16 [51]. However, a rather difficult analysis of their altitude dependence has shown that these inhomogeneities were apparently observed mostly in the lower part of the outer ionosphere. It is interesting to note that the spectrum has three maxima at ~ 1—3 km, 7—10 km, and 12—30 km. The maximum in the ~ 12—30 km region has a steep front, which possibly indicates that the excitation of these inhomogeneities has a resonant, shock-like character. A preliminary analysis of the possible types of waves associated with these inhomogeneities shows that these can be ion-cyclotron or Alfven waves. However, there are no experimental data on the frequency spectra of the plasma for these observations. It is also important to note that the electron density in the smaller inhomogeneities reaches 10^5—10^6 el/cm^3, i.e., ΔN is commensurate with or larger than the perturbed density N_0. This indicates that the excitation of the inhomogeneities in these cases is intense.

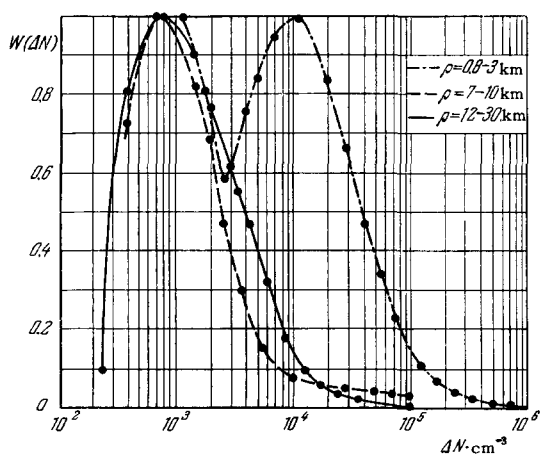

FIG. 16

We can indicate that the presence of inhomogeneous formations with dimensions 100—500 km up to altitudes of 700—1000 km has been established by different investigations. These data, however, are still skimpy. For the altitudes of interest to us, however, which extend to the border of the ionosphere, there are in general no measurement results at all.

5. IONIZATION BALANCE EQUATION IN THE OUTER IONOSPHERE

The general picture of the structure of the ionosphere, as considered above, indicates that a contemporary theory of ionosphere formation and the ionization-balance equation should be based on an allowance of a number of new important circumstances. These are dictated by the latest experimental data.

It is necessary, first, to bear in mind that the motion of the particles as in many cases non-Maxwellian. In a number of regions of the ionosphere the quasi-neutrality can apparently be violated ($N_e \neq N_i$), the plasma is not isothermal ($T_e \neq T_i$), and electric fields may be produced. In addition, it is not excluded that besides the formation of charged particles, due to ionization by the incident radiation (principally ultraviolet radiation from the sun), there is an influx of particles from the magnetosphere ("spilling" of particles) caused on by currents whose dynamics in the ionosphere can be quite complicated. As a net result, the ionization balance of the ionosphere should be based on a kinetic analysis and is solved self-consistently with the Poisson equation. Thus, the initial functions for the solution of the problem of the formation of the ionosphere should be the following: the altitude dependence of the particle distribution function, of the particles, of the electric and magnetic fields, and of the directional velocity of the particle motion.

All these functions, naturally, can be obtained essentially only by experiment.

On the other hand, the ionization-balance equation can be obtained from the kinetic equation in the following manner.* We have for one species of particles:

$$\frac{\partial f}{\partial t} + \mathbf{v}\frac{\partial f}{\partial \mathbf{r}} + \frac{e\mathbf{E}}{m}\frac{\partial f}{\partial \mathbf{v}} + \frac{e}{mc}[\mathbf{v}\,\mathbf{H}_0]\frac{\partial f}{\partial v} = \left\{\begin{matrix}\text{particle}\\ \text{formation}\end{matrix}\right\} + \left\{\begin{matrix}\text{particle}\\ \text{annihilation}\end{matrix}\right\} + \left\{\begin{matrix}\text{particle influx}\\ \text{from outside}\end{matrix}\right\}, \quad (25)^*$$

*The author is grateful to L. P. Pitaevskii for a discussion of this question.

*$[\mathbf{v}\,\mathbf{H}_0] \equiv \mathbf{v} \times \mathbf{H}_0$.

where $f(\mathbf{v}, \mathbf{E}_0, \mathbf{H}_0)$ is the distribution function and $\mathbf{v}$ is the summary velocity ({"thermal"} + {translational}).

We integrate (25) term by term, and obtain

$$\int_{-\infty}^{\infty} \frac{\partial f}{\partial t} d^3v = \frac{\partial}{\partial t} \int_{-\infty}^{\infty} f\, d^3v = \frac{\partial N}{\partial t}$$

which is the change in the density with time. Calculation of

$$\int_{-\infty}^{\infty} \mathbf{v} \frac{\partial f}{\partial \mathbf{r}} d^3v = \frac{\partial}{\partial \mathbf{r}} \int_{-\infty}^{\infty} \mathbf{v} f\, d^3v = \frac{\partial}{\partial \mathbf{r}} (\overline{N\mathbf{v}}) = \operatorname{div} (\overline{N\mathbf{v}})$$

yields the particle transport in general form. Further,

$$\int_{-\infty}^{\infty} \mathbf{E} \frac{\partial f}{\partial \mathbf{v}} d^3v = \mathbf{E} \int_{-\infty}^{\infty} \frac{\partial f}{\partial \mathbf{v}} d^3v = \mathbf{E} \int_{-\infty}^{\infty} \operatorname{grad}_{\mathbf{v}} f\, d^3v = \mathbf{E} \oint_{S_{\mathbf{v}}} \mathbf{n}_0 f\, dS_v = 0,$$

where $dS_{\mathbf{v}}$ is a surface element in velocity space, and $f \to 0$ when $v_\infty \to \infty$. Finally,

$$\int_{-\infty}^{\infty} [\mathbf{v}\,\mathbf{H}_0] \frac{\partial f}{\partial \mathbf{v}} d^3v = \int_{-\infty}^{\infty} \frac{\partial}{\partial \mathbf{v}} \{[\mathbf{v}\,\mathbf{H}_0] f\}\, d^3v - \int_{-\infty}^{\infty} f \frac{\partial}{\partial \mathbf{v}} [\mathbf{v}\,\mathbf{H}_0]\, d^3v$$

$$= \int_{S_{\mathbf{v}}} \mathbf{n}_0 \{[\mathbf{v}\,\mathbf{H}_0] f\}\, dS_{\mathbf{v}} - \int_{-\infty}^{\infty} \{\mathbf{H} \operatorname{curl} \mathbf{v} - \mathbf{v} \operatorname{curl} \mathbf{H}\} f\, d^3v = 0,$$

where $\mathbf{n}_0$ is the normal to the surface $S_{\mathbf{v}}$ in velocity space, and account is taken of the fact that

$$\frac{\partial}{\partial \mathbf{v}} [\mathbf{v} \times \mathbf{H}_0] = \operatorname{div}_{\mathbf{v}} [\mathbf{v} \times \mathbf{H}_0] \text{ and } f \to 0 \text{ when } v \to \infty,$$

while $\operatorname{curl} \mathbf{H}_0 = 0$ and $\operatorname{curl} \mathbf{v} = 0$.

As a result of these simple manipulations we obtain a system of ionization-balance equations in primary form

$$\begin{aligned} &\frac{\partial N_e}{\partial t} \quad \operatorname{div} (\overline{N\mathbf{v}})_e = I - \alpha N_e N_i - \beta N_e n + \left\{ \begin{matrix} \text{particle} \\ \text{influx} \end{matrix} \right\}, \\ &\frac{\partial N_i}{\partial t} \quad \operatorname{div} (\overline{N\mathbf{v}})_i = I - \alpha N_e N_i. \end{aligned} \tag{26}$$

However, it is necessary to add to (26) the equation

$$\nabla^2 \varphi = \operatorname{div} (N_e - N_i), \tag{27}$$

bearing in mind here that the conditions $N_i \sim N_e = N_{0e} e(e\varphi/\kappa T)$ can be satisfied.

We see, and this is the main conclusion of the analysis presented here, that to solve the system (26)—(27) we must know the quantities

$$\begin{aligned} (\overline{N\mathbf{v}})_e &= \int \mathbf{v}_e f_e\, d^3v, \qquad (\overline{N\mathbf{v}})_i = \int \mathbf{v}_i f_i\, d^3v, \\ N_e &= \int f_e\, d^3v, \qquad N_i = \int f_i\, d^3v, \end{aligned} \tag{28}$$

i.e., primarily the distribution functions. For concreteness, we assume in (26) that the formation of the particles

$$I \sim \sigma n \frac{S_\infty}{(h\nu)}, \tag{29}$$

i.e., the ionization) is due to incident ultraviolet radiation (n—density of neutral particles), and that the annihilation of particles is via photorecombination and electron adhesion.

[1] L. R. O. Storey, Phil. Trans. Roy. Soc. **A246**, 113 (1953).

[2] G. Allcok, J. Atmosph. Terr. Phys. **14**, 158 (1958).

[3] R. L. Smith, J. Geophys. Res. **66**, 3710 (1961).

[4] L. R. O. Storey, Ann. de Géophys. **14**, 144 (1958).

[5] D. L. Carpenter, J. Geophys. Res. **67**, 135 (1962); **68**, 1675 (1963); **71**, 693 (1966).

[6] J. J. Angerami, D. Carpenter, Report on Equatorial Aeronomy, p. 311 (1965); J. Geophys. Res. **71**, 711 (1966).

[7] H. B. Liemohn, F. L. Scarf, J. Geophys. Res. **69**, 883 (1964).

[8] H. Guthart, Radio Science **69D**, 1417 (1965).

[9] D. A. Gurnett, S. D. Shawhan, N. M. Brice, R. L. Smith, J. Geophys. Res. **70**, 1965; **71**, 741 (1966).

[10] K. I. Gringauz, Iskusstvennye sputniki Zemli (Artificial Earth Satellites), No. 12, 105 (1961); see also Patent No. 27, Byulleten' izobreteniĭ (Invention Bulletin), No. 12, 1964.

[11] K. L. Bowles, J. Res. Nat. Bur. Stand **65D**, 1 (1961).

[12] D. T. Farley, K. L. Bowles, NBS Report, 8489 (1964).

[13] J. V. Evans, J. Geophys. Res. **67**, 4914 (1962).

[14] G. P. Serbu, K. Maier, NBS Report, 8824 (1965); Space Research 5, 564 (1964).

[15] V. I. Slysh, Kosm. issl (Space Research) **3**, 760 (1965).

[16] R. C. Sagalyn, M. Smiddy, J. Geophys. Res. **69**, 1809 (1964).

[17] R. C. Sagalyn, M. Smiddy, Preprint (1965).

[18] Ya. L. Al'pert and V. M. Sinel'nikov, Geomagn. i aéronom. **5**, 209 (1965); Plan. Space Sci. **14**, 313 (1966).

[19] V. A. Misyura, G. K. Solodovnikov, and V. M. Migunov, Kosm. issl. **3**, 595 and 604 (1965).

[20] V. G. Istomin, Issledovaniya kosmicheskogo prostranstva (Investigations of Outer Space), Trans. All-union Conf. on Space Physics (Moscow, June 10—16, 1965), Nauka, 1965, p. 192.

[21] H. A. Taylor, H. G. Brinton, C. R. Smith, Preprint, Godard Space Flight Center (1965); J. Geophys. Res. **70**, 5769 (1965).

[22] V. G. Kurt, op. cit.[20], p. 576.

[23] J. P. Maclure, Equatorial Aeronomy, p. 170 (1965).

[24] V. C. Pineo, D. P. Hynek, G. H. Millman, J. Geophys. Res. **68**, 9695 (1963).

[25] K. L. Bowles, Space Research, p. 253, 1963.

[26] R. A. Goldberg, J. Geophys. Res. 70, 655 (1965).

[27] K. C. W. Champion, Air Force Surveys in Geophysics, N 164 (1965).

[28] Ya. L. Al'pert, Rasprostranenie radiovoln i ionosfera (Propagation of Radio Waves and the Ionosphere), Fizmatgiz 1960; Consultants Bureau, 1962.

[29] G. A. Mikhaĭlova, Geomagn. i aéronom. **2**, 257 (1963); **5**, 183 and 179 (1965).

[30] D. S. Fligel', ibid. **2**, 886 (1962).

[31] R. L. Smith et al., Nature **204**, 274 (1964).

[32] S. D. Shawhan, J. Geophys. Res. 71, 29 (1966).
[33] S. D. Shawhan, D. A. Gurnett, J. Geophys. Res. 71, 46 (1966).
[34] D. A. Gurnett, S. D. Shawhan, J. Geophys. Res. 71, 741 (1966).
[35] N. M. Brice, R. L. Smith, Nature 203, 926 (1964).
[36] J. S. Belrose, R. E. Barrington, Nature 203, 926 (1964).
[37] D. A. Gurnett, B. J. Brien, J. Geophys. Res. 69, 65 (1964).
[38] F. L. Scarf, G. M. Crook, R. W. Fredericks, J. Geophys. Res. 70, 3045 (1965).
[39] W. E. Gordon, Proc. JRE 46, 1824 (1958).
[40] K. L. Bowles, Phys. Rev. Letts. 1, 454 (1958).
[41] J. A. Fajer, Canad. J. Phys. 38, 1114 (1960); 39, 716 (1961).
[42] D. T. Farley, J. D. Dougherty, D. W. Barron, Proc. Roy. Soc. A263, 238 (1961).
[43] A. N. Akhiezer et al. Kollektivnye kolebaniya plazmy (Collective Plasma Oscillations), Atomizdat, 1964.
[44] I. Langmuir, H. M. Mott-Smith, General. Electric Rev. 27, 449, 538, 616, 762, 810 (1924); Phys. Rev. 28, 727 (1926).
[45] G. Hok, N. W. Spencer, W. G. Dow, J. Geophys. Res. 58, 235 (1953).
[46] Ya. L. Al'pert, A. V. Gurevich, and L. P. Pitaevskiĭ. Iskusstvennye sputniki v razrezhennoĭ plazme (Artificial Satellites in a Rarefied Plasma), Nauka, 1964; Space Physics with Artificial Satellites, Consultants Bureau, 1965.
[47] Ya. L. Al'pert, Geomagn. i aéronom. 5, 3 (1965); Space Sci. Rev. 4, 373 (1965).
[48] A. V. Gurevich, L. V. Pariiskaya, and L. P. Pitaevskii, JETP 49, 647 (1965), Soviet Phys. JETP 22, 449 (1966).
[49] Ya. L. Al'pert, UFN 49, No. 1 (1953); JETP 21, 38 (1961).
[50] J. A. Ratcliffe, Rep. Progr. Physics 19, 188 (1957).
[51] E. A. Benediktov, G. G. Getmantsev, N. A. Mityakov, V. O. Rapoport, Yu. A. Sazonov, and A. F. Tarasov, op. cit. [20], p. 581.
[52] R. W. Knecht, T. E. Van Zant, Nature 197, 641 (1963).
[53] J. W. King, Proc. Roy. Soc. A281, 464 (1964).
[54] J. O. Thomas, A. Y. Sader, J. Geophys. Res. 69, 4561 (1964).
[55] A. K. Paul, J. W. Wright, J. Geophys. Res. 69, 1431 (1964).
[56] T. J. Daynarsh, W. W. Farley, J. Geophys. Res. 70, 5361 (1965).
[57] T. M. Watt, J. Geophys. Res. 70, 5849 (1965).
[58] R. E. Barrington, J. S. Belrose, G. L. Nelms, J. Geophys. Res. 70, 1647 (1965).
[59] D. B. Muldrew, J. Geophys. Res. 70, 2635 (1965).
[60] Ya. L. Al'pert, L. N. Vitshas, and V. M. Sinel'nikov, Geomagn. i aéron. 5, 649 (1965).
[61] G. P. Serbu, K. Maier, Goddard Space Flight Center, X-615-66-92, 1966.
[62] T. Obayashi, Report Ion. Space Res. Japan 19, 214 (1965).

Translated by J. G. Adashko